HHS Public Access

Author manuscript

J Pharm Sci. Author manuscript; available in PMC 2022 April 07.

Published in final edited form as:

J Pharm Sci. 2021 April ; 110(4): 1693–1700. doi:10.1016/j.xphs.2020.10.046.

Affinity-based polymers provide long-term immunotherapeutic drug delivery across particle size ranges optimal for macrophage targeting

Nathan A. Rohner[1], **Linda N. Purdue**[1], **Horst A. von Recum**[1]

[1]Department of Biomedical Engineering, Case Western Reserve University, 10900 Euclid Avenue, Cleveland, OH 44106

Abstract

Drug delivery to specific arms of the immune system can be technically challenging to provide prolonged drug release while limiting off-target toxicity given the limitations of current drug delivery systems. In this work, we test the design of a cyclodextrin (CD) polymer platform to extend immunomodulatory drug delivery via affinity interactions for sustained release at multiple size scales. The parameter space of synthesis variables influencing particle nucleation and growth (pre-incubation time and stirring speed) and post-synthesis grinding effects on resulting particle diameter were characterized. We demonstrate that polymerized CD forms exhibit size-independent release profiles of the small molecule drug lenalidomide (LND) and can provide improved drug delivery profiles versus macro-scale CD polymer disks in part due to increased loading efficiency. CD polymer microparticles and smaller, ground particles demonstrated no significant cytotoxicity as compared to the base CD monomer when co-incubated with fibroblasts. Uptake of ground CD particles was significantly higher following incubation with RAW 264.7 macrophages in culture over standard CD microparticles. Thus, the affinity/structure properties afforded by polymerized CD allow particle size to be modified to affect cellular uptake profiles independently of drug release rate for applications in cell-targeted drug delivery.

Keywords

Controlled release; immunotherapy; cyclodextrin(s); injectable(s); microparticle(s); particle size; polymer synthesis

Corresponding Author: Horst A. von Recum, 10900 Euclid Ave, Cleveland, OH 44106, Tel: (216) 368-5513; Fax: (216) 368-4969; horst.vonrecum@case.edu.

Disclosures

H.A. von Recum is a co-founder of Affinity Therapeutics but does not receive salary. The other authors have nothing to disclose.

Supporting Information

Further supporting information is available online. Supplementary table S1 demonstrates the effect of stir speed on resulting particle diameters and PDI. Supplementary table S2 shows the effect of pre-polymerization time on resulting particle diameters and PDI. Supplementary table S3 details effect of base pre-polymer choice on resulting particle diameters and PDI. Supplementary figure S1 demonstrates the physical characteristics of the different types of CD microparticles synthesized.

1. Introduction

Sustained, localized lenalidomide (LND) delivery is not clinically available, yet could improve patient outcomes and reduce associated costs for many chronic disease scenarios. LND is used clinically to treat multiple myeloma and chronic lymphocytic leukemia and has shown promise in pre-clinical studies for other chronic and debilitating diseases. However, the frequent, often daily treatments, especially due to rising drug prices, cost up to $14,656 per patient per month for multiple myeloma in 2014[1]. Chronic lymphocytic leukemia costs patients in the U.S. $5.13 billion annually; and the per-patient lifetime cost is over $600,000, with oral targeted therapies becoming the first-line of treatment[2]. Despite the monetary costs, there are major benefits to LND therapy for multiple myeloma and chronic lymphocytic leukemia patients. Subjects with chronic lymphocytic leukemia treated with LND experience a longer period of progression-free survival (median 33.9 months)[3]. Moreover, current clinical studies illustrate that LND can extend time to subsequent treatment without affecting the ability of a patient to respond to subsequent therapy[4]. In the case of multiple myeloma, patients treated with LND exhibited a 15% 8-year overall survival increase in comparison to the placebo group[5]. Adding even more potential for this small molecule drug with multiple mechanisms of action, LND treatment of Parkinson's disease and multiple sclerosis has demonstrated benefits in pre-clinical animal models[6,7]. With a total cost each year of $25 billion, Parkinson's treatment is in need of better options as for a patient in long-term care, the annual cost is approximately $15,000–30,000[8]. Multiple sclerosis costs $2.5 billion in the United States, with lifetime costs for patients exceeding $4 million[9].

In clinical applications, repeated oral administration of LND is needed due to a half-life of bioavailability of approximately 3 hours[2]. LND has proven to be beneficial, but current therapy is wasteful, expensive and requires continuous dosing that relies heavily upon patient compliance and exhibits some concern for off-target effects. Oral LND doses deliver very little to the target cells as most of the dosage is excreted[2,5]. LND also demonstrates poor solubility, increasing the difficulty of successfully delivering high concentrations to the area of treatment. In previous work, we have leveraged polymerized cyclodextrins (pCD) to continuously deliver hydrophobic, small molecule drugs on the order of weeks to months by leveraging affinity interactions[10–21]. This method utilizes a high concentration of affinity complexation sites to delay drug release by polymerizing CD monomers into larger disk structures, coatings, and more[11–13,22–26]. Herein, the synthesis variables for polymerizing CD microparticles and the resulting device size effects are explored for reducing CD-associated cytotoxicity, providing sustained LND delivery with a single application, and promoting cellular uptake *in vitro*.

2. Materials and Methods

2.1 Materials

α-cyclodextrin (α-CD) prepolymer, β-cyclodextrin (β-CD) prepolymer, γ-cyclodextrin (γ-CD) prepolymer, lightly crosslinked with epichlorohydrin, and octakis (6-deoxy-6-amino) γ-CD octahydrochloride were purchased from CycloLab (Budapest, Hungary). Ethylene glycol diglycidyl ether was purchased from Polysciences, Inc. (Warrington, PA).

Hexamethylene diisocyanate was purchased from Sigma-Aldrich (St. Louis, MO). LND was purchased from Cayman Chemicals (Ann Arbor, MI). All other reagents, solvents, and chemicals were purchased from Thermo Fisher Scientific (Waltham, MA).

2.2 Methods

2.2.1 Microparticle Synthesis—Synthesis began with either epichlorohydrin-crosslinked α-CD, β-CD, or γ-CD prepolymer solubilized in 0.2 M potassium hydroxide (25% w/v) and pre-heated to 60°C for 20 minutes. A 50:1 light mineral oil to Tween85/Span85 solution (24%/76%) was mixed on a stir plate at 60°C. Ethylene glycol diglycidyl ether was added drop-wise to the solution. Next, the solution was vortexed to ensure homogenous distribution of the crosslinker before being poured into the oil/Tween85/Span85 mixture. Temperature was then increased to 70°C. After three hours, the polymerized CD microparticles were formed. The microparticles were centrifuged to get rid of excess oil, washed with excess hexanes twice, and finally washed with deionized water twice. The microparticles were resuspended, frozen, and lyophilized until dry before further use. β-CD particles were used to provide consistency among methods in experiments for validating synthesis parameter effects on size, evaluating grinding time effects, and determining viability, yet similar results are achievable with the other CD prepolymers. γ-CD polymer (selected due to its predicted greater affinity binding (66.5±22.5 μM) with LND) was tested in LND release and macrophage uptake studies to demonstrate application.

2.2.2 Polydispersity Index (PDI) Calculations—A glass micrometer scale was imaged to calculate the pixel to distance conversion factor in ImageJ using the straight segmented line tool[27]. Microparticle sizes were calculated by measuring the diameter in pixels and converting to microns. The average (non-weighted) diameters were calculated from at least 40 individual particle measurements from 2–3 batches per condition. The PDI of the synthesized microparticles was calculated by dividing the standard deviation by the size average and then squaring the resulting value. The PDI expresses uniformity of the synthesized particles in solution.

2.2.3 Scanning Electron Microscope Imaging—Samples were prepared by gold sputter coating after mounting to the SEM (scanning electron microscope) stage with carbon tape. Images were taken using a JSM-6510LV SEM (JEOL USA, Peabody, MA) under high vacuum with a 15kV accelerating voltage at a working distance of 14 mm and scan time of 20 seconds. Magnification and scale bars are as indicated in the figure captions and images.

2.2.4 Particle Grinding—Polymerized microparticles were transferred into a porcelain mortar. Pestle grinding in a consistent, circular motion was continued for a pre-determined time period. Deionized water was added to the mortar, and the solution pipetted out with multiple washes ensuring maximal recovery of the ground particle population.

2.2.5 Disk Synthesis—To make polymer disks for comparison to γ-CD particles, vacuum dried epichlorohydrin-crosslinked γ-CD prepolymer was dissolved in dimethylsulfoxide (DMSO) as a 25% w/v solution and heated. 1,6-hexamethylene diisocyanate (HDI) was added to the solution and then vortexed. Bubbles were removed

by gentle stirring. The homogenous solution was poured into a Teflon dish, covered with parafilm, and allowed to crosslink until it completely solidified. The polymer film was cut into disks using an 8mm circular biopsy punch. The resulting disks were washed in sequence with excess DMSO for 24 hours, then a 50/50 solution of DMSO and deionized water the next day, and finally deionized water alone with daily replacement for 3 days before drying.

2.2.6 Viability and Proliferation Assay—National Institute of Health NIH/3T3 fibroblasts (ATCC.org, Manassas, VA) were cultured in Dulbecco's Modified Eagle's Medium (DMEM) supplemented with fetal bovine serum (FBS) and penicillin/streptomycin at 37°C with 5% CO_2. Cells were plated at 50,000 cells per well in a 24 well tissue culture treated plate and allowed to adhere in media. Autoclave sterilized β-CD polymer microparticles, ground β-CD particles, or β-CD monomer were added either directly to the cell wells or into 0.4 micron cutoff well inserts (Thermo Fisher Scientific, Waltham, MA) at equivalent concentrations of 50 μg/mL, and incubated for 72 hours. Cells in media with no CD or pCD particles incubated concurrently were used as positive control wells. 100 μl of 0.15 mg/ml resazurin (Thermo Fisher Scientific, Waltham, MA), was added to evaluate metabolic activity in the alamarBlue assay for quantifying fibroblast viability and proliferation[28], per treatment well. After incubation for an additional 24 hours, fluorescence at 530/590 nm was measured with a Synergy H1 Microplate Reader (BioTek Instruments, Inc., Winooski, VT) and results were normalized to media only controls.

2.2.7 LND Drug Loading and Release—This release tested three polymer size conditions: γ-CD disks, standard γ-CD microparticles, and ground γ-CD microparticles. Each condition was composed of three sample tubes, each containing 20 mg of polymer. To account for any possible drug remaining in the tube, a control aliquot that did not contain any CD was used as baseline. A stock loading solution of LND in DMSO was made at 10 mg/mL. Each sample tube received 1 mL of loading solution and the polymers were allowed to complex with the LND for 3 days. During the loading period and throughout the release, the sample tubes were kept on a shaker with a regulated temperature of 37°C. After the loading period concluded, loading solutions were replaced with release buffer (1x Dulbecco's Phosphate-Buffered Saline with 0.1% Tween80, which acts as a physiological buffer providing a hydrophobic sink[16,29]). At pre-determined time points of 1, 3, 24, 48 and every 24 hours thereafter up to 432 hours, a sample of release media was taken for analysis. The aliquots were then centrifuged down and the excess solution was pipetted off carefully to ensure no removal of polymers, followed by complete replacement of the release buffer. LND was measured via fluorescence signal at 251 excitation and 409 emission wavelengths in release aliquots using a Synergy H1 Microplate Reader. Fluorescence signals were converted to concentrations using a standard curve from known LND dilutions.

2.2.8 Macrophage Particle Uptake—RAW 264.7 macrophages were cultured in DMEM supplemented with FBS and penicillin/streptomycin at 37°C with 5% CO_2. The cells were seeded onto cover slips and allowed to adhere before addition of rhodamine-labeled γ-CD microparticles and γ-CD ground particles into culture media. Samples were gently agitated to mix and cells were allowed to incubate with the particle suspensions for 72 hours. Cover slips were then washed 3x in PBS before fixing in 4% paraformaldehyde

and mounted with Vectashield (Vector Laboratories, Inc., Burlingame, CA) on glass slides for imaging with a Zeiss Observer.Z1 microscope equipped with an AxioCam ERc5s (Carl Zeiss AG, Oberkochen, Germany).

2.2.9 Statistical Analysis—Data are represented as the mean with standard deviation or standard error of the mean where specified. Statistics were calculated using GraphPad Prism 8 software (GraphPad Software, La Jolla, CA). Statistical significance was defined as $p < 0.05$ following appropriate statistical tests with post-hoc information noted in the figure captions.

3. Results

3.1 Microparticle Synthesis Setup Allows for Critical Parameter Control

The need for new multi-functional biomaterials is evident given the resistances and barriers to conventional therapeutic approaches for many diseases. The use of polysaccharide-based polymers as biomaterial depots and in functional coatings for the delivery of small molecule drugs, such as antibiotics and anti-inflammatory therapeutics has seen steady improvement[11,13,18,20,30,31]. Previously, polymerized CDs (pCD) were leveraged to continuously deliver small molecule drugs on the order of weeks to months by leveraging affinity interactions[10,11,16,19–21,25,30,32,33]. However, a variety of particle sizes may be necessary for targeting different tissues and cellular subtypes[34,35]. Current batch synthesis of CD polymer particles is accomplished via inverse emulsion polymerization and sizing is performed with microscopy (Figure 1).

3.2 Stir Speed and Pre-Polymerization Time Effects on CD Particle Size

During CD particle synthesis, applicable parameters were varied to determine impact on the size of the polymerized particles. The speed of the stirring was first altered during a constant three hour synthesis time. Stir speeds of 300–1000 RPM still resulted in feasible particle polymerization, while slower speeds did not form particles. Stir speed is an important factor, since too slow of mixing results in polymer micelle coagulation and sedimentation that inhibits proper polymer microsphere formation. It was determined that increased stirring speed resulted in smaller polymerized particles (Figure 2A, Supplementary Table S1). These results are consistent with previous reports for emulsion and inverse emulsion polymerization reactions[36,37], in part due to the increased kinetic energy from faster stirring increasing the probability of polymer chains colliding in solution, thus increasing particle nucleation. As more reactant is used in generating new particles, less is available as the reaction proceeds to grow particles, resulting in smaller overall diameters. The effect of pre-polymerization before starting the reverse emulsion polymerization with stirring was also tested during microparticle synthesis. Crosslinker was added and the solution was vortexed, but was not poured into the oil/Tween85/Span85 mixture until the indicated time. The range of feasible pre-polymerization time included 0–120 minutes. It was found that as the length of pre-polymerization time increased, the size of the polymerized CD microparticles also increased up to 60 minutes; yet, a 120 minute period of pre-polymerization resulted in smaller particles possibly due to decreased crosslinker reaction efficiency (Figure 2B, Supplementary Table S2).

3.3 CD Polymer Particles Exhibit Robust Stability

The polymerized particles synthesized from alpha, beta, and gamma monomer-derivatives were compared to one another. Minor differences in size were measured between particles formed from the different CD types (Figure 3A, Supplementary Table S3). All CD types generated similar-shaped spherical microparticles as exhibited in Supplementary Figure 1. To test pH effects on particle size and stability, especially important for the tumor microenvironment[38], polymerized β-CD microparticles were exposed to a range of pH between 4 and 10. It was found that despite the wide range in pH, the microparticles demonstrated no significant change in size (Figure 3B). Polymerized microparticles were also sonicated, which has been traditionally used to break up particle clumps that are not thoroughly crosslinked. Tubes containing the microparticles were placed in a bath sonication machine, which applied sonic waves to the particles. Different sonication times were tested, from 1–60 minutes, but resulted in no significant change in microparticle size (data not shown).

3.4 Polymeric β-CD Particle Size Alterable Post-Synthesis

Traditional particles, liposomes, and shell-core drug delivery systems require changes in synthesis to modify physical parameters and are even then limited in size modifications. However, it was hypothesized that polymerized CD would be amenable to post-processing techniques due to the homogenous polymeric crosslinking structure while still maintaining effective release profiles via their affinity-based release mechanism. To determine if microparticle size could be altered post-synthesis, microparticles were ground for a pre-determined amount of time using a mortar and pestle. They were ground for either one, five, or ten minutes. Samples of each time point were taken, and it was determined that while one minute did not significantly reduce pCD particle diameters, five and ten minutes of grinding reduced the average particle diameter to 61% and 36% of original size, respectively (Figure 4A). Moreover, SEM images of dried ground CD particles depicted an overall spherical shape (Figure 4B).

3.5 CD Polymer Particles Exhibit No Adverse Cytotoxicity as Compared to Monomer

Previous studies have indicated that CD monomer has a potential cytotoxic effect, sequestering cholesterol and other molecules from the body[39]. Polymerized CD microparticles and smaller ground particles were co-incubated with NIH/3T3 cells for 24 hours and proliferation and viability was determined relative to cells in media with neither CD nor pCD particles (media+cells positive control wells). We chose to use β-CD in this experiment as it exhibited the greatest cytotoxic potential in previous research[39]. Interestingly, we found pCD-β-MP and ground pCD-β-MP exhibited excellent cytocompatibility whether in direct incubation or separated from cells via a 0.4 micron pore-size transwell filter (Figure 5). However, the β-CD monomer was observed to reduce proliferation of cells by almost 60% after 24 hours incubation (Figure 5).

3.6 CD Polymer Macrostructures Extend LND Drug Release

Synthesized CD particles were prepared and loaded with LND for 72 hours followed by release into buffer. Drug loading efficiency was calculated by dividing the total amount of

LND loaded into polymers (determined via fluorescence of leeched drug and compared to a standard curve) by the drug amount in the initial loading solution and presented as mean with standard deviation. The drug loading efficiency for pCD-disks was 12.3 ± 3%, pCD-γ-MP was 43.3 ± 5.7%, and ground pCD-γ-MP was 39.5 ± 4.5%. These results indicate the enhanced drug loading offered by the increased surface area to volume ratio of the polymer microparticles versus the larger depot-style disks, thus allowing for increased drug diffusion and loading into the hydrophobic binding pockets of the pCD. Daily release aliquots were measured with complete replacement of release buffer. We observed similar release profiles from both standard pCD microparticles and smaller, ground pCD microparticles; with longer continuous release and less burst release than larger pCD implantable depots (8 mm diameter disks). While pCD disks exhibited LND release for an average 7.3 days, the pCD-γ-MP and ground particle forms continuously released LND for an average of 11.7 and 12 days, respectively (Figure 6B).

3.7 RAW 264.7 Macrophages Primarily Uptake Ground CD Particles

Ground and standard pCD-γ-MP were synthesized with a small percentage of rhodamine fluorescently tagged CD and incubated with RAW 264.7 macrophages in culture for 72 hours to assess particle uptake by cells. There was significantly increased particle uptake observed with the smaller size ground particles, but almost none for the standard pCD-γ-MP, (Figure 7A). Fluorescent signal from particles conjugated with dye and associated with cells after thorough washing was averaged per image using ImageJ (Figure 7B). These results indicate a smaller particle size for internalization may be key for association with macrophages and targeted drug delivery.

4. Discussion

This study demonstrates the process for polymer microparticle synthesis via inverse emulsion and the effect of relevant parameters on resulting particle diameters (Figures 1 and 2). An excellent review on understanding and controlling emulsion polymerization highlights the importance of the particle nucleation and growth effects on size distributions[37]. Different CD pre-polymers showed a similar particle size for α-CD and β-CD, while γ-CD microparticles were significantly smaller by statistical comparison, while the biological relevance of this specific size difference is yet to be determined (Figure 3). This effect could result from more potential binding sites on the larger CD molecules resulting in a denser overall polymer structure for pCD-γ-MP. Polymerized CD particles exhibit robustness to pH changes and sonication, yet particle diameter can be impacted by mortar and pestle grinding (Figure 4). Particle size was significantly smaller after 5 and 10 minutes of grinding, but not statistically significant between the two grinding times. Expanding these findings to research applications, we show that the monomer, but not the polymer version of CD is cytotoxic *in vitro* (Figure 5), and agrees with previous results for CD monomer cytotoxicity[40]. Rather than a burst of drug being delivered, CD polymer slowly releases the LND in physiological conditions for an extended period of up to 12 days (Figure 6), due to the ability of γ-CD to form a drug inclusion complex of high affinity with LND, allowing binding kinetics to mediate sustained release rather than polymer degradation over time. Moreover, the increased surface area of the microparticles resulted

in increased loading efficiency and therefore significantly extended drug delivery versus the larger (8 mm) polymer disks. Other studies have demonstrated extended drug release profiles by combining CD with chitosan into smaller nanoparticles, indicating potential for improving function by including additional materials[41]. Further advantage of the CD polymer particle system is demonstrated in grinding particles to smaller sizes amenable to increased cellular uptake as observed with macrophages (Figure 7). Overall, our results indicate CD particle size modification can be performed independent of changing the drug release rate of the system for future applications in tissue or cellular passive targeting of hydrophobic drugs.

Targeted and sustained delivery options for LND are needed, as evidenced by trials of treatment cycles. Previously, two separate trials were conducted to analyze the impact of LND treatment doses and cycles for multiple myeloma. The IFM 2005–02 study ran two 28 day cycles, where subjects were given 25 mg/day of LND on days 1–21 of the cycle. The mean time of treatment was 25 months, which was then followed by maintenance treatment within the six months following autologous stem-cell transplantation. Once a day, 10 mg of LND were given to the subject for the first three months of maintenance treatment. If the subject did not have a dose-limiting toxicity, the dosage was increased to 15 mg. For the second trial, CALGB 100104, mean initial treatment time was extended to 30 months. It followed the same procedure for maintenance treatment as the IFM 2005–02 study, but maintenance was started 100–110 days after ASCT[5]. The CONTINUUM trial was conducted to determine the effects of treating chronic lymphocytic leukemia with LND. For the first 28 day cycle, the subject received 2.5 mg of LND once a day. If this dose was well tolerated, the second 28 cycle was increased to a 5 mg dose per day. The dosage was increased to 10 mg per day only if five continuous cycles of 5 mg/day were well tolerated and they had not received a minimal residual disease negative complete response[3,4]. LND also required frequent dosing in animal models, exploring the possible treatment of Parkinson's disease. The dosing schedule was found to have protective effects for amyotrophic lateral sclerosis. The solution containing LND was made fresh every week, and was administered via oral gavage five times a week in a 5 mL/kg volume[6]. Furthermore, LND was tested therapeutically in an animal model of multiple sclerosis (MS) exhibiting experimental autoimmune encephalomyelitis (EAE). After the appearance of clinical symptoms, 30 mg/kg in 0.9% CMC-Na of LND was administered daily to the mice[7]. Additional factors further hinder LND efficacy as LND has poor solubility; 82% of the administered dose is excreted unchanged in the urine[5] and it is unable to penetrate the blood-brain barrier (BBB) effectively, especially when compared to its parent molecule thalidomide[6]. Further efforts in drug delivery system development for LND may overcome these barriers to maximize therapeutic effects.

LND indicates potential for targeting numerous pathways with the greatest impacts on the polarization of macrophages, switching from M1, proinflammatory, to M2, anti-inflammatory. When the polarization of M2 macrophages is promoted, proinflammatory Th1 and Th17 cells in the peripheral lymph system and central nervous system (CNS) are subsequently inhibited. The polarization also indirectly alters proinflammatory activity of myelin-specific CD-4$^+$ T cells, including IFN-γ^+ and IL17$^+$ cell subtypes[7]. The expression levels of pro-inflammatory cytokines, such as TNF-α, interferon γ, IL-1β, and IL-6,

are also reduced[6]. LND also increases the expression and autocrine secretion of the anti-inflammatory cytokine IL-10[7]. Following LND treatment, the levels of anti-inflammatory cytokine IL-13 are found to be elevated[6]. Thus far, the treatment of LND has only been delivered through oral doses, yet the benefit for selective LND localization to certain tissues and cellular subtypes is unknown. Future applications could include co-delivery of LND with other drugs for increased therapeutic effect, such as daratumumab, dexamethasone[42], and rituximab to treat mantle-cell lymphoma or mucosa-associated lymphoid tissue (MALT) lymphoma[43,44].

Supplementary Material

Refer to Web version on PubMed Central for supplementary material.

Acknowledgements

The authors would like to acknowledge support from NIH T32DK083251 (NAR), R01GM12147-03 (HvR), and from an NIH Research Facilities Construction Grant (C06 RR12463-01).

References

1. Fonseca R, Abouzaid S, Bonafede M, Cai Q, Parikh K, Cosler L, Richardson P 2017. Trends in overall survival and costs of multiple myeloma, 2000–2014. Leukemia 31(9):1915–1921. [PubMed: 28008176]
2. Chen N, Zhou S, Palmisano M 2017. Clinical Pharmacokinetics and Pharmacodynamics of Lenalidomide. Clinical pharmacokinetics 56(2):139–152. [PubMed: 27351179]
3. Chanan-Khan A, Egyed M, Robak T, Martinelli de Oliveira FA, Echeveste MA, Dolan S, Desjardins P, Blonski JZ, Mei J, Golany N, Zhang J, Gribben JG 2017. Randomized phase 3 study of lenalidomide versus chlorambucil as first-line therapy for older patients with chronic lymphocytic leukemia (the ORIGIN trial). Leukemia 31(5):1240–1243. [PubMed: 28140392]
4. Chanan-Khan AA, Zaritskey A, Egyed M, Vokurka S, Semochkin S, Schuh A, Kassis J, Simpson D, Zhang J, Purse B, Foa R 2017. Lenalidomide maintenance therapy in previously treated chronic lymphocytic leukaemia (CONTINUUM): a randomised, double-blind, placebo-controlled, phase 3 trial. The Lancet Haematology 4(11):e534–e543. [PubMed: 28958469]
5. Syed YY 2017. Lenalidomide: A Review in Newly Diagnosed Multiple Myeloma as Maintenance Therapy After ASCT. Drugs 77(13):1473–1480. [PubMed: 28791622]
6. Valera E, Mante M, Anderson S, Rockenstein E, Masliah E 2015. Lenalidomide reduces microglial activation and behavioral deficits in a transgenic model of Parkinson's disease. J Neuroinflammation 12:93–93. [PubMed: 25966683]
7. Weng Q, Wang J, Wang J, Wang J, Sattar F, Zhang Z, Zheng J, Xu Z, Zhao M, Liu X, Yang L, Hao G, Fang L, Lu QR, Yang B, He Q 2018. Lenalidomide regulates CNS autoimmunity by promoting M2 macrophages polarization. Cell Death Dis 9(2):251–251. [PubMed: 29445144]
8. Fredericks D, Norton JC, Atchison C, Schoenhaus R, Pill MW 2017. Parkinson's disease and Parkinson's disease psychosis: a perspective on the challenges, treatments, and economic burden. The American journal of managed care 23(5 Suppl):S83–s92. [PubMed: 28715903]
9. Hartung DM, Bourdette DN, Ahmed SM, Whitham RH 2015. The cost of multiple sclerosis drugs in the US and the pharmaceutical industry: Too big to fail? Neurology 84(21):2185–2192. [PubMed: 25911108]
10. Wang NX, von Recum HA 2010. Affinity-Based Drug Delivery. Macromolecular Bioscience 11(3):321–332. [PubMed: 21108454]
11. Cyphert EL, von Recum HA 2017. Emerging technologies for long-term antimicrobial device coatings: advantages and limitations. Experimental Biology and Medicine 242(8):788–798. [PubMed: 28110543]

12. Cyphert EL, Zuckerman ST, Korley JN, von Recum HA 2017. Affinity interactions drive post-implantation drug filling, even in the presence of bacterial biofilm. Acta Biomaterialia 57:95–102. [PubMed: 28414173]
13. Rohner NA, Dogan AB, Robida OA, von Recum HA 2019. Serum biomolecules unable to compete with drug refilling into cyclodextrin polymers regardless of the form. Journal of materials chemistry B 7(35):5320–5327.
14. Edgardo R-D, Zhina S, Nick XW, Jonathan K, Sapna S, Michael K, Chris F, Adonis ZH, Horst AvR 2016. Local release from affinity-based polymers increases urethral concentration of the stem cell chemokine CCL7 in rats. Biomedical Materials 11(2):025022. [PubMed: 27097800]
15. Rivera-Delgado E, Djuhadi A, Danda C, Kenyon J, Maia J, Caplan AI, von Recum HA 2018. Injectable liquid polymers extend the delivery of corticosteroids for the treatment of osteoarthritis. Journal of Controlled Release 284:112–121. [PubMed: 29906555]
16. Rivera-Delgado E, Nam JK, von Recum HA 2017. Localized Affinity-Based Delivery of Prinomastat for Cancer Treatment. ACS Biomaterials Science & Engineering 3(3):238–242. [PubMed: 33465922]
17. Rivera-Delgado E, Sadeghi Z, Wang N X, Kenyon J, Satyanarayan S, Kavran M, Flask C, Hijaz A Z, von Recum H A 2016. Local release from affinity-based polymers increases urethral concentration of the stem cell chemokine CCL7 in rats. Biomedical Materials 11(2):025022. [PubMed: 27097800]
18. Rivera-Delgado E, von Recum HA 2017. Using Affinity To Provide Long-Term Delivery of Antiangiogenic Drugs in Cancer Therapy. Molecular Pharmaceutics 14(3):899–907. [PubMed: 28128564]
19. Haley RM, Qian VR, Learn GD, von Recum HA 2019. Use of affinity allows anti-inflammatory and anti-microbial dual release that matches suture wound resolution. Journal of biomedical materials research Part A 107(7):1434–1442. [PubMed: 30771234]
20. Haley RM, von Recum HA 2018. Localized and targeted delivery of NSAIDs for treatment of inflammation: A review. Experimental Biology and Medicine:1535370218787770.
21. Haley RM, Zuckerman ST, Gormley CA, Korley JN, von Recum HA 2019. Local delivery polymer provides sustained antifungal activity of amphotericin B with reduced cytotoxicity. Experimental Biology and Medicine 244(6):526–533. [PubMed: 30897959]
22. Blatnik JA, Thatiparti TR, Krpata DM, Zuckerman ST, Rosen MJ, von Recum HA 2017. Infection prevention using affinity polymer-coated, synthetic meshes in a pig hernia model. Journal of Surgical Research 219:5–10.
23. Grafmiller KT, Zuckerman ST, Petro C, Liu L, von Recum HA, Rosen MJ, Korley JN 2016. Antibiotic-releasing microspheres prevent mesh infection in vivo. Journal of Surgical Research 206(1):41–47.
24. Cyphert EL, Learn GD, Hurley SK, Lu C-y, von Recum HA 2018. Bone Cements: An Additive to PMMA Bone Cement Enables Postimplantation Drug Refilling, Broadens Range of Compatible Antibiotics, and Prolongs Antimicrobial Therapy (Adv. Healthcare Mater. 21/2018). Advanced Healthcare Materials 7(21):1870080.
25. Juric D, Rohner NA, von Recum HA 2019. Molecular Imprinting of Cyclodextrin Supramolecular Hydrogels Improves Drug Loading and Delivery. Macromolecular Bioscience 19(1):1800246.
26. Rohner NA, Schomisch SJ, Marks JM, von Recum HA 2019. Cyclodextrin Polymer Preserves Sirolimus Activity and Local Persistence for Antifibrotic Delivery over the Time Course of Wound Healing. Mol Pharm 16(4):1766–1774. [PubMed: 30807185]
27. Schneider CA, Rasband WS, Eliceiri KW 2012. NIH Image to ImageJ: 25 years of image analysis. Nature Methods 9(7):671–675. [PubMed: 22930834]
28. Voytik-Harbin SL, Brightman AO, Waisner B, Lamar CH, Badylak SF 1998. Application and evaluation of the alamarBlue assay for cell growth and survival of fibroblasts. In vitro cellular & developmental biology Animal 34(3):239–246. [PubMed: 9557942]
29. Jhunjhunwala S, Balmert SC, Raimondi G, Dons E, Nichols EE, Thomson AW, Little SR 2012. Controlled Release Formulations of IL-2, TGF-β1 and Rapamycin for the Induction of Regulatory T Cells. Journal of controlled release : official journal of the Controlled Release Society 159(1):78–84. [PubMed: 22285546]

30. Halpern JM, von Recum HA. 2014. Affinity-based delivery systems. In Ma PX, editor Biomaterials and Regenerative Medicine, ed., Cambridge: Cambridge University Press. p 419–430.

31. Rohner NA, Thomas SN 2017. Flexible Macromolecule versus Rigid Particle Retention in the Injected Skin and Accumulation in Draining Lymph Nodes Are Differentially Influenced by Hydrodynamic Size. ACS Biomater Sci Eng 3(2):153–159. [PubMed: 29888321]

32. Fu AS, Thatiparti TR, Saidel GM, von Recum HA 2011. Experimental Studies and Modeling of Drug Release from a Tunable Affinity-Based Drug Delivery Platform. Annals of Biomedical Engineering 39(9):2466–2475. [PubMed: 21678091]

33. Halpern JM, Gormley CA, Keech M, von Recum HA 2014. Thermomechanical Properties, Antibiotic Release, and Bioactivity of a Sterilized Cyclodextrin Drug Delivery System. Journal of materials chemistry B, Materials for biology and medicine 2(18):2764–2772. [PubMed: 24949201]

34. Palao-Suay R, Aguilar MR, Parra-Ruiz FJ, Martin-Saldana S, Rohner NA, Thomas SN, San Roman J 2017. Multifunctional decoration of alpha-tocopheryl succinate-based NP for cancer treatment: effect of TPP and LTVSPWY peptide. Journal of materials science Materials in medicine 28(10):152. [PubMed: 28861765]

35. Palao-Suay R, Martin-Saavedra FM, Rosa Aguilar M, Escudero-Duch C, Martin-Saldana S, Parra-Ruiz FJ, Rohner NA, Thomas SN, Vilaboa N, San Roman J 2017. Photothermal and photodynamic activity of polymeric nanoparticles based on alpha-tocopheryl succinate-RAFT block copolymers conjugated to IR-780. Acta Biomater 57:70–84. [PubMed: 28511874]

36. Valot P, Baba M, Nedelec JM, Sintes-Zydowicz N 2009. Effects of process parameters on the properties of biocompatible Ibuprofen-loaded microcapsules. International Journal of Pharmaceutics 369(1):53–63. [PubMed: 19084583]

37. Lovell PA, Schork FJ 2020. Fundamentals of Emulsion Polymerization. Biomacromolecules.

38. Zhang X, Lin Y, Gillies RJ 2010. Tumor pH and its measurement. Journal of nuclear medicine : official publication, Society of Nuclear Medicine 51(8):1167–1170.

39. Stella VJ, He Q 2008. Cyclodextrins. Toxicologic pathology 36(1):30–42. [PubMed: 18337219]

40. Szente L, Singhal A, Domokos A, Song B 2018. Cyclodextrins: Assessing the Impact of Cavity Size, Occupancy, and Substitutions on Cytotoxicity and Cholesterol Homeostasis. Molecules 23(5):1228.

41. Zhao L, Tang B, Tang P, Sun Q, Suo Z, Zhang M, Gan N, Yang H, Li H 2020. Chitosan/Sulfobutylether-β-Cyclodextrin Nanoparticles for Ibrutinib Delivery: A Potential Nanoformulation of Novel Kinase Inhibitor. Journal of Pharmaceutical Sciences 109(2):1136–1144. [PubMed: 31606544]

42. Dimopoulos MA, Oriol A, Nahi H, San-Miguel J, Bahlis NJ, Usmani SZ, Rabin N, Orlowski RZ, Komarnicki M, Suzuki K, Plesner T, Yoon SS, Ben Yehuda D, Richardson PG, Goldschmidt H, Reece D, Lisby S, Khokhar NZ, O'Rourke L, Chiu C, Qin X, Guckert M, Ahmadi T, Moreau P 2016. Daratumumab, Lenalidomide, and Dexamethasone for Multiple Myeloma. The New England journal of medicine 375(14):1319–1331. [PubMed: 27705267]

43. Ruan J, Martin P, Shah B, Schuster SJ, Smith SM, Furman RR, Christos P, Rodriguez A, Svoboda J, Lewis J, Katz O, Coleman M, Leonard JP 2015. Lenalidomide plus Rituximab as Initial Treatment for Mantle-Cell Lymphoma. The New England journal of medicine 373(19):1835–1844. [PubMed: 26535512]

44. Sidaway P 2017. Rituximab enhances responses to lenalidomide. Nature Reviews Clinical Oncology 14(2):70–70.

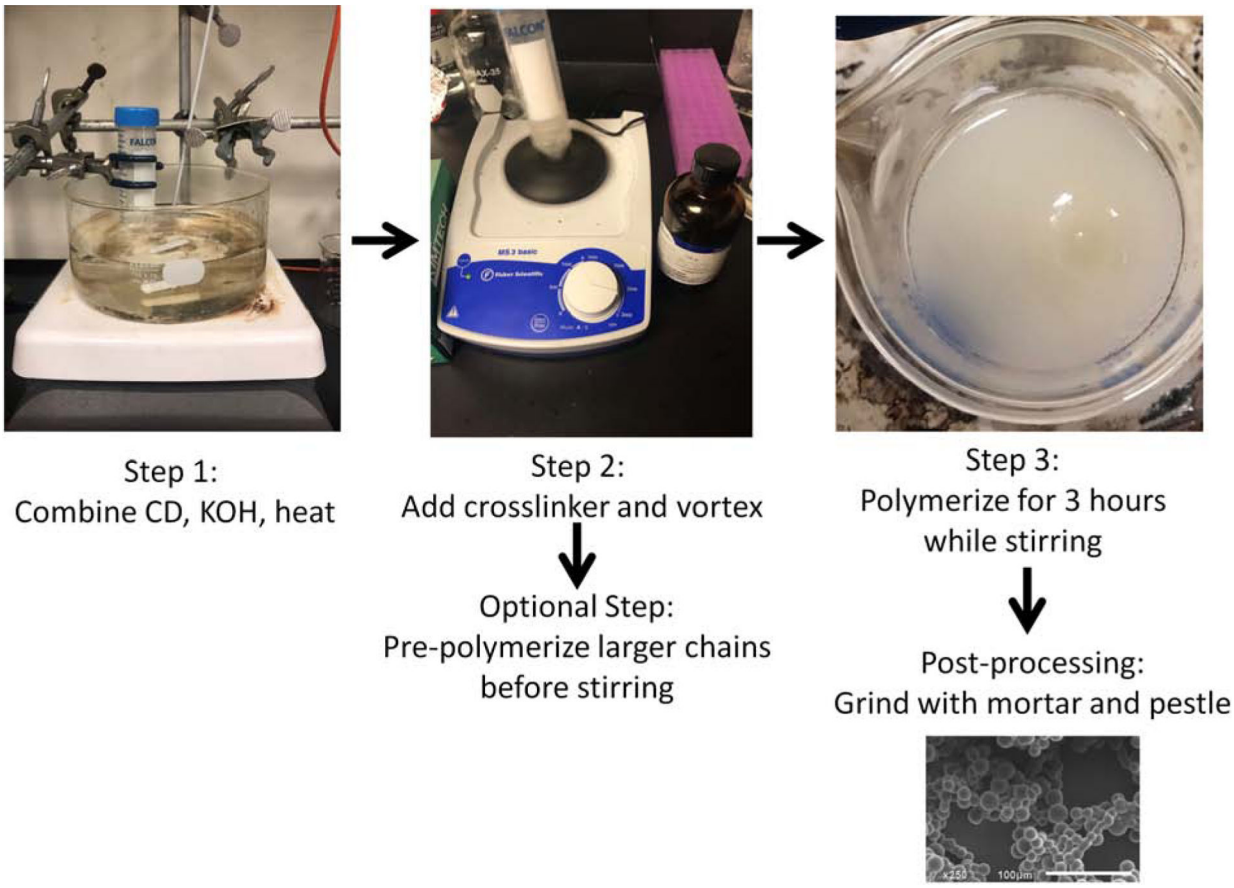

Figure 1.
Synthesis schematic and pictures depicting synthesis process. SEM image of ground particles.

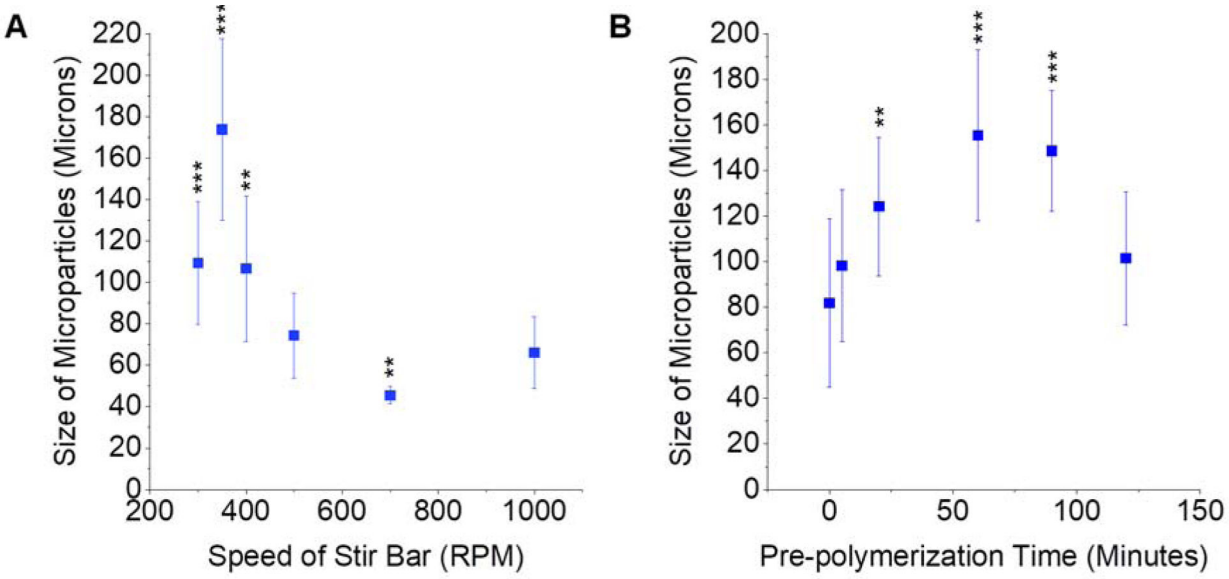

Figure 2.

Effect of modifying RPM (A) or pre-polymerization time (B) on CD particle size. * indicates $p < 0.05$, ** $p < 0.01$, *** $p < 0.001$ by one-way ANOVA followed by Bonferroni multiple comparisons versus the 500 RPM results (A) and the 0 minute pre-polymerization condition (B). n=2–3 batches per condition with at least 40 individual particles sized per batch. Error bars represent the standard deviation.

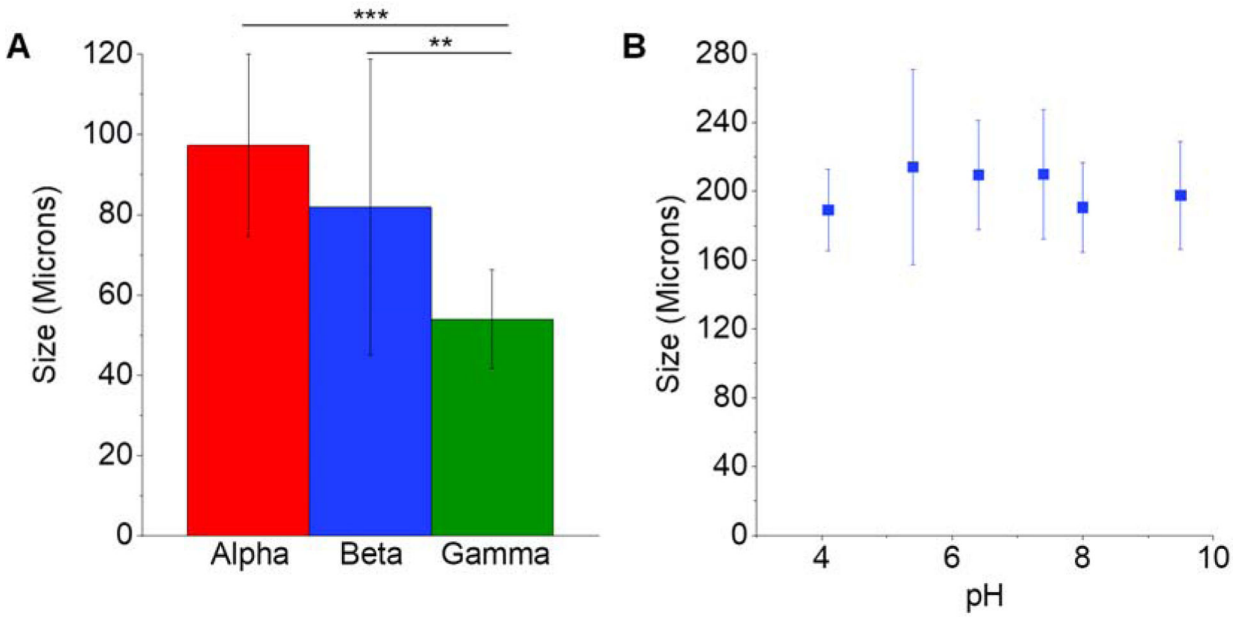

Figure 3.

Testing polymeric CD particle variations and robustness, we observe only minor changes in size when synthesized from various CD pre-polymer types (A). Particle size does not change significantly with change in pH from 4–10 (B). * indicates $p < 0.05$ by one-way ANOVA with Tukey post-hoc (A). n=3 batches per condition with at least 40 individual particles sized per batch. Error bars represent the standard deviation.

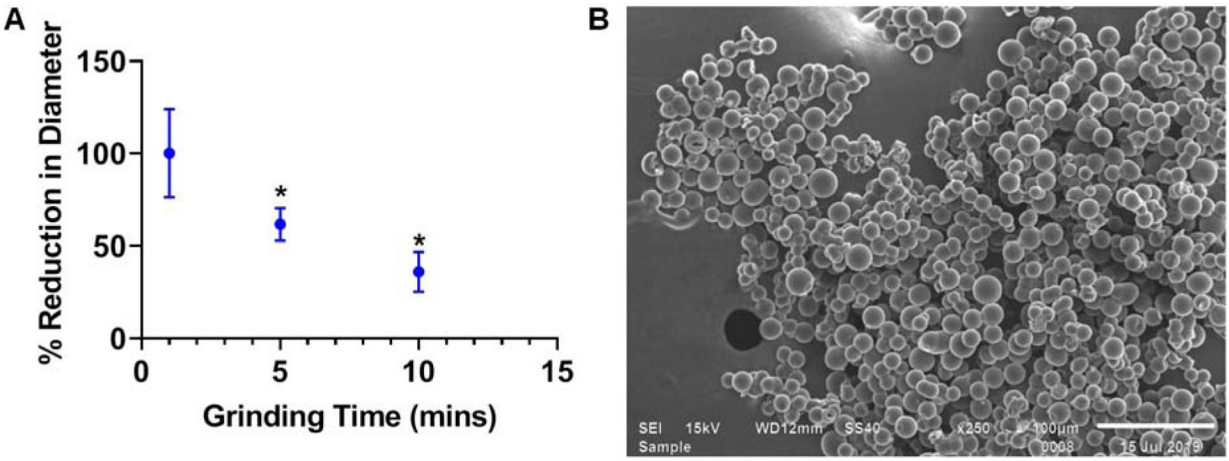

Figure 4.

Polymeric CD particle diameter changes upon grinding time with mortar and pestle with measurements of particles for samples at different time points (A). SEM images of dry, ground polymerized CD particles indicate surfaces are still geometrically spherical even after grinding (B). * indicates $p < 0.05$ by one-way ANOVA with Tukey post-hoc. n=3 replicates each. Error bars represent the standard deviation.

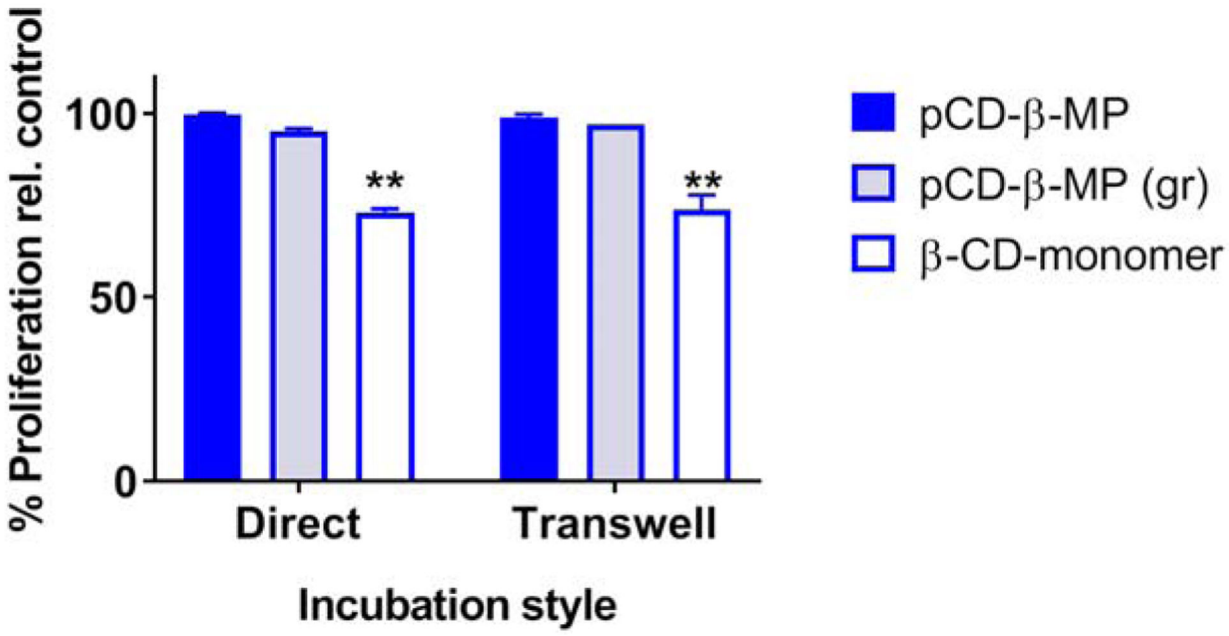

Figure 5.

Direct and indirect CD cytotoxicity to NIH/3T3 cells in co-culture with microparticles, ground particles, and CD monomer relative to untreated controls. The 0.4 micron transwell allows metabolites and CD monomer to pass through, but not particles. ** indicates $p < 0.01$ by two-way ANOVA with Tukey test post-hoc versus the healthy, normal growth of the control group; n=3 replicates each. Error bars represent the standard deviation.

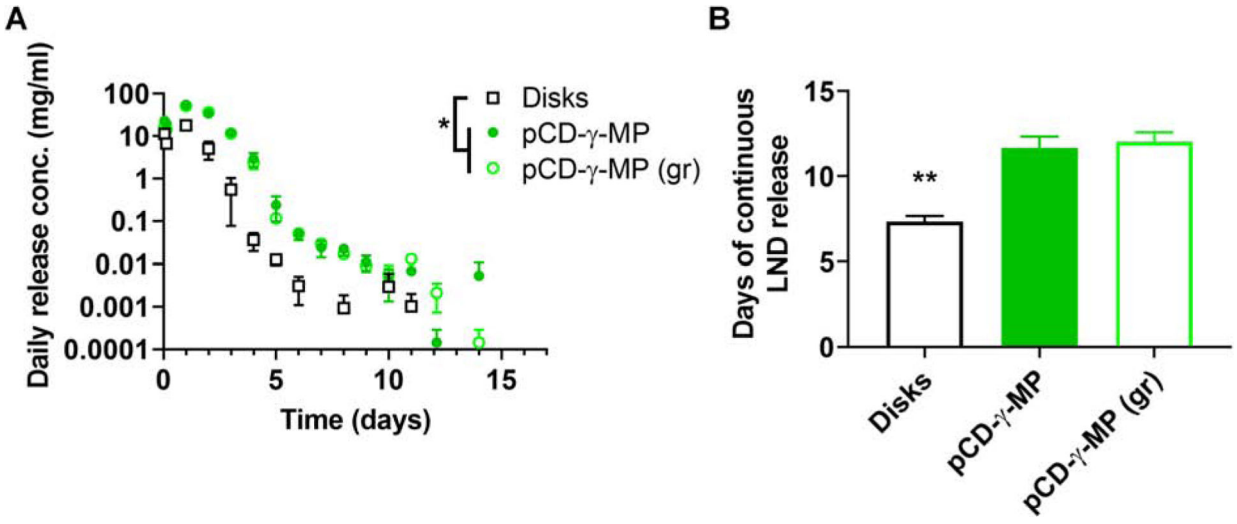

Figure 6.

Lenalidomide daily release profiles from pCD-γ-MP, pCD-γ-MP (ground), and γ-disks (A). Days of continuous non-zero release of LND from each formulation (B). * indicates $p < 0.05$ by two-way ANOVA with Tukey test post-hoc between the disks and both the pCD-γ-MP and pCD-γ-ground MP groups at 3–96 hours post-incubation (A) and by one-way ANOVA with Bonferonni post-hoc for cumulative days of release between the disks and both the pCD-γ-MP and pCD-γ-ground MP (B). n=3 replicates per condition. Error bars represent the standard error of the mean (A) and standard deviation (B).

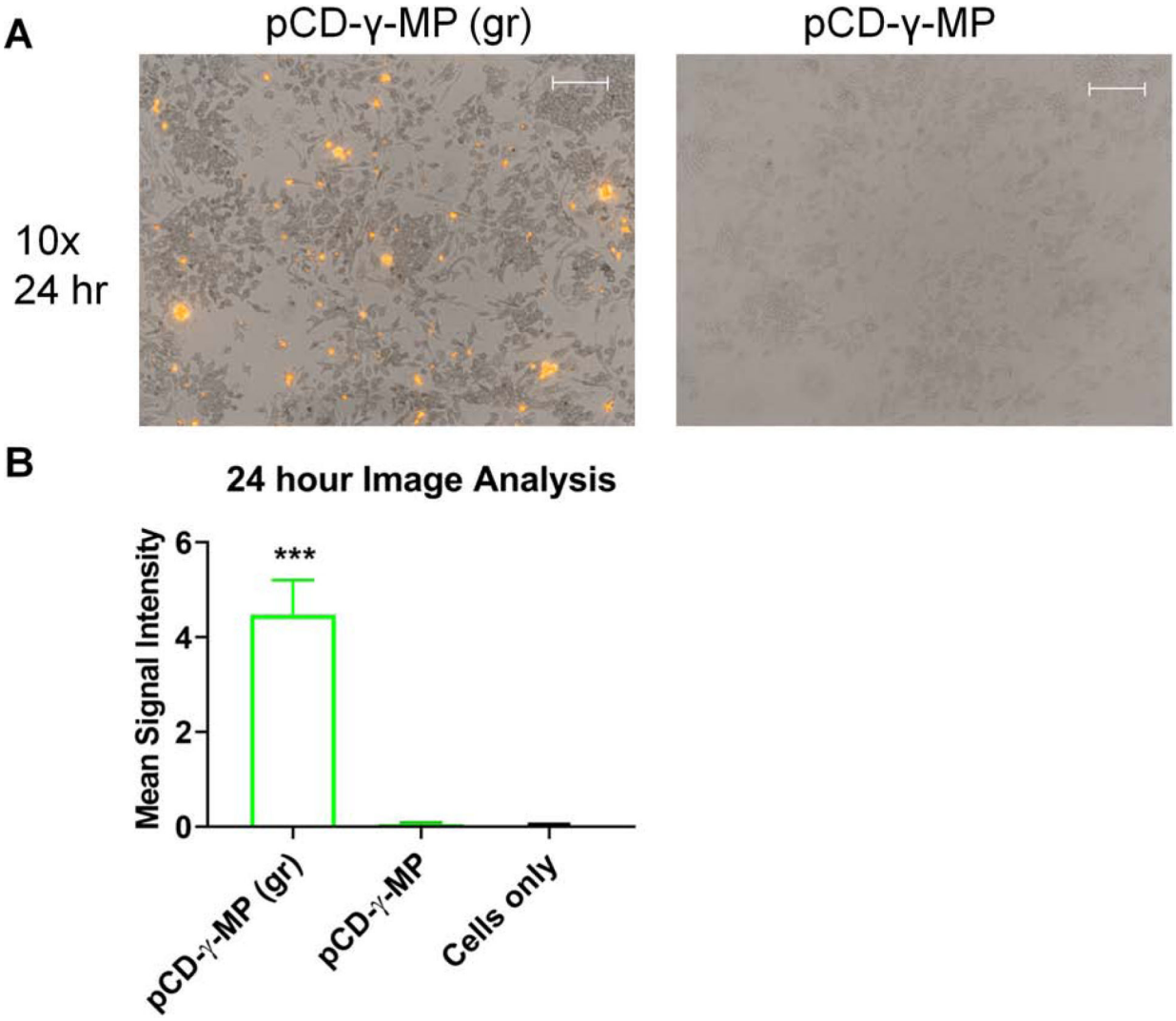

Figure 7.

The effect of particle size on macrophage uptake *in vitro* demonstrated by representative images (A) and averaged fluorescence signal data (B). Scale bars = 100 microns. *** indicates $p < 0.001$ by one-way ANOVA with Tukey test post-hoc. Average intensity from n=6–15 images per group. Error bars represent standard error of the mean.